Infection Regulates Pro-Resolving Mediators that Lower Antibiotic Requirements

Published in final edited form as:
Nature. ; 484(7395): 524–528. doi:10.1038/nature11042.

Infection Regulates Pro-Resolving Mediators that Lower Antibiotic Requirements

Nan Chiang[1], **Gabrielle Fredman**[1], **Fredrik Bäckhed**[2], **Sungwhan F. Oh**[1], **Thad Vickery**[1], **Birgitta A. Schmidt**[1], and **Charles N. Serhan**[1,§]

[1]Center for Experimental Therapeutics and Reperfusion Injury, Department of Anesthesiology, Perioperative and Pain Medicine, Harvard Institutes of Medicine, Brigham and Women's Hospital and Harvard Medical School, Boston, Massachusetts 02115, USA.

[2]Sahlgrenska Center for Cardiovascular and Metabolic Research/Wallenberg Laboratory, University of Gothenburg, SE-413 45 Gothenburg, Sweden.

Abstract

Underlying mechanisms for how bacterial infections contribute to active resolution of acute inflammation are unknown[1-4]. Here, we performed exudate leukocyte trafficking and mediator-metabololipidomics of murine peritoneal *Escherichia coli (E. coli)* infections with temporal identification of pro-inflammatory (prostaglandins and leukotrienes) and specialized pro-resolving mediators (SPM). In self-resolving *E. coli* exudates (10^5 CFU), the dominant SPM identified were resolvin (Rv) D5 and protectin D1 (PD1), which at 12 h were significantly greater than levels in exudates from higher titer *E. coli* (10^7 CFU) challenged mice. Germ-free mice displayed endogenous RvD1 and PD1 levels higher than in conventional mice. RvD1 and RvD5 (ng/mouse) each reduced bacterial titers in blood and exudates, *E. coli*-induced hypothermia and increased survival, demonstrating the first actions of RvD5. With human polymorphonuclear neutrophils (PMN) and macrophages, RvD1, RvD5, and PD1 each directly enhanced phagocytosis of *E. coli*, and RvD5 counter-regulated a panel of pro-inflammatory genes, including NF-κB and TNF-α. RvD5 activated the RvD1 receptor, GPR32, to enhance phagocytosis. With self-limited *E. coli* infections, RvD1 and the antibiotic ciprofloxacin accelerated resolution, each shortening resolution intervals (R_i). Host-directed RvD1 actions enhanced ciprofloxacin's therapeutic actions. In 10^7 CFU *E. coli* infections, SPM (RvD1, RvD5, PD1) together with ciprofloxacin also heightened host antimicrobial responses. In skin infections, SPM enhanced vancomycin clearance of *Staphylococcus aureus*. These results demonstrate that specific SPM are temporally and differentially regulated during infections and that they are anti-phlogistic, enhance containment and lower antibiotic requirements for bacterial clearance.

Correspondence and requests for materials should be addressed to cnserhan@zeus.bwh.harvard.edu.. [§]*Address correspondence and reprint requests to:* Center for Experimental Therapeutics and Reperfusion Injury, Department of Anesthesiology, Perioperative and Pain Medicine, Harvard Institutes of Medicine, Brigham and Women's Hospital and Harvard Medical School, MA 02115. Phone: 617-525-5001; Fax : 617-525-5017 cnserhan@zeus.bwh.harvard.edu.

Supplementary Information is linked to the online version of the paper at www.nature.com/nature.

Author Contributions NC, GBF & SFO contributed to experimental design, carried out experiments and data analyses. TV and SFO performed metabololipidomics and lipid mediator analyses. FB carried out experiments with germ-free mice and contributed to manuscript composition. BAS carried out dermatopathology. All authors contributed to manuscript presentation and figure preparation. NC and CNS carried out overall experimental design and CNS conceived of the overall research plan.

Author Information Reprints and permissions information is available at www.nature.com/reprints.

Competing Financial Interests C.N.S. is an inventor on patents [resolvins] assigned to BWH and licensed to Resolvyx Pharmaceuticals. C.N.S. is a scientific founder of Resolvyx Pharmaceuticals and owns equity in the company. C.N.S.' interests were reviewed and are managed by the Brigham and Women's Hospital and Partners HealthCare in accordance with their conflict of interest policies.

The acute inflammatory response is a protective mechanism that is evolved to eliminate invading organisms. It should ideally be self-limited and lead to complete resolution, returning to homeostasis[1-4]. Evidence has emerged indicating that resolution of acute inflammation is an active process with biosynthesis of specialized pro-resolving mediators (SPM), e.g. resolvins (recently reviewed[4,5]). During natural resolution, PMN required for anti-microbial defense[2] stop further infiltration, apoptose and are removed from the inflammatory site by specific macrophages (MΦ)[6-10]. In sterile inflammation, resolving exudates biosynthesize SPM from essential fatty acids including lipoxins (LX) from arachidonic acid, E-series resolvins (Rv) from omega-3 eicosapentaenoic acid (EPA), D-series Rv, protectins (PD) and maresins from docosahexaenoic acid (DHA) (reviewed in[4,11]). In humans, SPM production is also temporally regulated[12,13], and SPM selectively control inflammation by stimulating resolution without immunosuppression, and are organ protective in eye, kidney, lung and periodontal diseases[4,14].

Self-resolving E. coli infections versus higher titer E. coli challenges: *E. coli* infections are an urgent worldwide health concern as in a recent outbreak in Germany. In the United States, *E. coli* infections account for ~270,000 cases/year with underreporting estimated at ~20-fold[15]. Here we used a well-established model of murine peritonitis, relevant to human infections[16], to identify specific SPM that may be directly involved in resolving infections. *E. coli* inoculation at 10^5 CFU/mouse i.p. evoked a self-limited host response (Fig. 1a). PMN infiltration reached maximum at ~12 h followed by decline. Monocytes/MΦ gradually increased from 2 h to 72 h; most of the exudate mononuclear cells at later time points were MΦ (~90% CD14+F4/80+ cells; Fig. S1a), a finding consistent with anti-phlogistic actions of MΦ (e.g. clearing apoptotic PMN)[6,7]. To provide quantitative analysis of resolution components with *E. coli* infection, we used resolution indices[4], since they give unbiased assessment of progress during resolution and are now in wide use (*cf.* [9,17]). Resolution indices were T_{max} ~12h and T_{50} ~28h, giving a resolution interval (R_i) of 16h (see Methods). In sharp contrast, inoculation at 10^7 CFU/mouse delayed resolution with sustained PMN infiltration (Fig. 1b). PMN continued to increase until 72 hours and the major mononuclear cell type at later intervals was monocytes (~90 % CD14+F4/80−; Fig. S1a), with only ~6% MΦ. Also with the higher inoculum of 10^7 CFU, bacteria counts in both blood and lavages remained elevated at 24-48h, whereas with lower *E. coli* inoculum bacteria were cleared by 24h (Fig. S1b). Thus, high inoculum of 10^7 CFU evoked excessive PMN accumulation and limited MΦ in exudates that reflect delayed resolution of infection. Importantly, the lower *E. coli* inoculum gave self-limited profiles (R_i=16h), permitting differential analysis.

Infection-resolution metabololipidomics: Profiling metabololipidomics targeted on local acting lipid mediators (LM) was carried out with *E. coli* exudates using mass spectrometry-based LM-lipidomics targeting 5 LM metabolomes, e.g. leukotrienes, resolvins and protectins (Figs. 1c and S1). In self-resolving peritonitis (10^5 CFU), biosynthetic pathway markers for protectin D1 (PD1) and maresins (MaR1), namely 17-HDHA and 14-HDHA, were identified and elevated at the peak of PMN infiltration ~12h in resolving exudates (see Table S1 for LM identification). By comparison, mice that received higher titer *E. coli* (10^7 CFU) gave increased levels of proinflammatory LTB_4 and reduced 17-HDHA and 14-HDHA levels at 12-48h (Figs. 1c & S1d). Within the initial phase (4h), RvD5 (7*S*,17*S*-dihydroxy-docosa-4*Z*,8*E*,10*Z*,13*Z*,15*E*,19*Z*-hexaenoic acid), a pivotal biosynthetic marker[18] accumulated in self-resolving exudates (120±39 pg/exudate), ~3 times more than in exudates from higher titer *E. coli* infections (40±11 pg RvD5/exudates, $p<0.05$) (Figs. 1c & S1). At later interval 12h, RvD5 remained elevated (326±39 pg/exudate) in self-resolving exudates. It is noteworthy that PD1 levels were also significantly greater in self-resolving exudates (1066±247 pg/exudate) than in higher titer *E. coli*-challenged (468±116 pg/exudate). In these exudates, RvD5 and PD1 were most abundant of the DHA metabolome.

Human PMN transform 17-H(p)DHA via two distinct biosynthetic pathways to RvD5 and/or PD1 (Fig. S2)[4,18]. These pathways were activated on infection and utilized endogenous essential fatty acids without supplement to biosynthesize potent novel mediators (*vide infra*). Their presence suggested specific role(s) in resolving infection.

RvD5 and PD1 each accumulated while RvD1 rapidly disappeared in exudates from *E. coli* infections. To monitor metabolic flux of RvD1 during *E. coli* infections, RvD1 was administered with *E. coli* (10^5 CFU) into peritoneum (Fig. S3a). At 12-24h post-inoculation, only 5-10% RvD1 was recovered from peritoneal exudates. Along these lines, with human macrophages ~40-50% of RvD1 was lost within 0.5-2.0 h accompanied by an increase in its further metabolite dihydro-RvD1. (Fig. S3b). Hence, these are dynamic pathways in infectious exudates.

We calculated ratios for pro-resolving vs. inflammatory mediators, i.e. RvD5/LTB_4 and PD1/LTB_4. In self-resolving exudates these ratios at 12 and 24h were greater than those in exudates from higher (10^7 CFU) *E. coli* infections (Fig. S1e), indicating that differential LM exudate profiles were present with these *E. coli* infections. To access their potential endogenous roles, we profiled these pathways in germ-free mice[19] (Fig. 1d). In colons of naive germ-free mice, lower amounts of LTB_4 were identified and increased levels of endogenous DHA products 14-HDHA, 17-HDHA, RvD1, as well as PD1 (Figs. 1e&f, S4). Hence, both endogenous and infected tissues produced D-series resolvins and PD1.

Since D-series resolvins, in particular RvD5, were one of the more abundant SPM, we sought to determine its impact in *E. coli* infections. RvD5 given in physiologic range, i.e. nanograms/mouse with *E. coli* (10^7 CFU) significantly enhanced phagocyte containment of *E. coli in vivo* (160% increase) compared to mice challenged with *E. coli* alone (Fig. 2a). RvD1 shared this action, registering 42% increase. Of note, RvD1 or RvD5 markedly reduced blood and exudate bacterial counts (Fig. 2b). Infected mice developed hypothermia, giving 2.4±1.2°C decrements in body (surface) temperature. Both RvD1 and RvD5 prevented this (Fig. 2c&S5a). The higher lethal dose *E. coli* (2.5×10^7 CFU) gave only 25% survival) and RvD1 significantly increased survival to ~66% (Figs. 2d and S5b, $p<0.05$). Here, RvD5 significantly reduced pro-inflammatory cytokines KC and TNFα in exudates and RvD1 decreased IL-1β (Fig. S5c). Thus, both RvD1 and RvD5 stimulated phagocyte *E. coli* ingestion, lowered bacterial titers, protected from hypothermia and increased survival.

Given these *in vivo* findings, we next questioned whether SPM have a direct impact on bacterial containment with isolated human cells. RvD1, RvD5 and PD1 each potently enhanced human MΦ phagocytosis of fluorescent *E. coli* ~40-70% increases in pM to nM ranges (Fig. 3a-c). We also tested whether RvD5 activates human RvD1 receptor GPR32 expressed in a beta-arrestin reporter system[20], and found that RvD5 directly activates this receptor (Fig. S6a). RvD5-enhanced phagocytic activity also proved dependent on GPR32. Both RvD1 and RvD5 increased MΦ phagocytosis of *E. coli*, an action further enhanced with GPR32 overexpression compared to mock transfected cells (Fig. S6b).

Gene array analysis with human MΦ (> 90 genes) showed that *E. coli* up-regulated a panel of inflammation-related genes, including NF-κB, phosphodiesterase 4B (PDE4B), COX-2 (PTGS2) and TNFα. These results are consistent with Gram-negative lipopolysaccharide (LPS) stimulation of MΦ that up-regulates COX-2[21], phosphodiesterase 4B (PDE4B) and TNFα[22]. When RvD5 (1 nM) was incubated with MΦ and *E. coli*, many of these genes were down-regulated. RvD1 down-regulated, e.g., PDE4B and COX-2 (Fig. 3d and Table S2). Ablation of PDE4B protects mice from LPS-induced septic shock[23] and inhibition of COX enhances bacterial clearance of penicillin-resistant *Streptococcus pneumoniae*[24]. Therefore, RvD1 and RvD5 each counter-regulate COX and proinflammatory signaling components

initiated by *E. coli* that might contribute to their actions in enhancing non-phlogistic phagocytosis (Fig. 3, Table S2) and bacterial clearance *in vivo* (Fig. 2).

Similar findings were obtained with human PMN, where RvD1, RvD5 and PD1 each stimulated PMN anti-microbial mechanisms, increasing *E. coli* ingestion and intracellular reactive oxygen species (ROS) production for killing during *E. coli* challenge (Fig. S7). These SPM did not exhibit direct anti-bacterial activities (Fig. S8). Together, these results characterize anti-phlogistic and antibacterial actions of RvD5, RvD1 and PD1 in that they enhance phagocytic activity of human phagocytes without evoking pro-inflammatory responses of these cells.

SPM and antibiotics: Antibiotic-resistant bacteria are a global concern, increasing health-care costs. Ciprofloxacin, for example, is the only antibiotic recommended by the World Health Organization for management of bloody diarrhea[25]. Unfortunately, rapid increases in bacterial resistance to ciprofloxacin reduces treatment options[25]. Hence, new strategies are needed. Given that specific SPM enhanced bacterial containment (Figs. 2, 3), we questioned whether SPM-directed host responses would embellish antibiotic treatment. To this end, we determined resolution indices for ciprofloxacin and RvD1. Given along with *E. coli* (10^5 CFU), RvD1 (50 ng) reduced maximal PMN (Ψmax), and shortened resolution interval (R_i) from ~20h to ~12h (Fig. 4a). Ciprofloxacin alone at equi-doses also reduced R_i to ~11h and initiated resolution at an earlier point Tmax ~6h. RvD1 plus ciprofloxacin further accelerated the onset of resolution with Tmax ~4h, and reduced R_i to ~5h (Fig. 4a and Table S3).

RvD1 plus ciprofloxacin further reduced bacterial titers in blood and exudates at 4h, compared to ciprofloxacin alone (Fig. 4b). Similar results were obtained at 12h with exudates, whereas there were no significant differences between Cipro and Cipro plus RvD1 in blood. RvD1 actions were more pronounced at 4h in blood. A panel of cytokines/chemokines was monitored (Fig. S9A), and RvD1 and ciprofloxacin each gave differential actions; RvD1 significantly reduced IL-1β, IL-6 and increased IL-10 at 4h, and IFNγ at 24h. Ciprofloxacin alone reduced IL-12 levels at 4h (Fig. S9B). We also assessed LM metabololipidomic profiles: RvD1 plus ciprofloxacin significantly increased both 14-HDHA and PD1 at 4h (Figs. 4c, S9C&D), whereas neither alone was effective. At 12h, RvD1 or ciprofloxacin alone increased endogenous PD1. In addition, RvD1 or ciprofloxacin alone at 4 h did not enhance macrophage containment of *E. coli*, but significantly increased phagocytic activity when both were administered (Fig. S9E). Thus, host-directed RvD1 responses plus bacteria-directed antibiotic accelerated resolution via enhanced *E. coli* killing and clearance, as well as selectively regulated both endogenous LM and cytokines.

Since the specific SPM identified in infectious exudates were from DHA metabolome (Fig. 1), we tested RvD1, RvD5 and PD1 together (50 ng each) plus ciprofloxacin (25 μg/mouse) in higher titer *E. coli* (10^7 CFU) infections. Sub-optimal doses of ciprofloxacin (25 μg, Fig. S10A) still protected mice from hypothermia and reduced bacterial titers, actions that were enhanced by the SPM panel (Fig. 4d). In addition, treatment with both ciprofloxacin and SPMs significantly increased phagocyte ingestion of *E coli*, whereas neither treatment alone proved effective (Fig. S10B).

SPM enhance actions of vancomycin in S. aureus-initiated infections: *Staphylococcus aureus* is an emerging cause of various skin infections and a high percentage of hospital-acquired infections are caused by antibiotic-resistant *S. aureus*[25]. To assess a second system, we determined the impact of SPM and vancomycin in *S. aureus*-initiated infections in murine dorsal skin pouches. SPM panel (RvD1, RvD5 and PD1, 100 ng each) and/or sub-optimal doses of vancomycin (2.5 μg) were administrated with *S. aureus* (10^5 CFU) via

intra-pouch injections. SPM or vancomycin alone at 4h each decreased exudate bacterial counts by ~10-fold. Treatment with both further reduced bacterial counts by ~100-fold (Fig. S11 A,B). Similar results were obtained at 24 h; SPM and vancomycin together gave significantly lower bacterial counts compared to those from each treatment alone (Fig. 4e). In *S. aureus*-infected mice, histologic analysis demonstrated PMN infiltration and Gram stain positives within linings surrounding the pouch cavities (Figs. 4f & S11c) that were markedly reduced by SPM, vancomycin and their use together (Fig. 4f).

A panel of cytokines/chemokines was also monitored. SPM and vancomycin at 4h significantly reduced *S. aureus*-induced IL-6 and GM-CSF in pouch exudates (Fig. S11), whereas neither alone was effective. It is noteworthy that vancomycin reduced LTB_4 and increased the Rv precursor 17-HDHA (Fig. S11). Other SPM, including resolvin E1, protect mice from *E. coli* pneumonia and acute lung injury[26] and 15-epi-LXA_4, an arachidonic acid-derived SPM, enhances resolution of *E. coli* pulmonary inflammation[27] and macrophage phagocytosis[28]. Hence, it appears that specific SPM pathways are used by the host during Gram-positive and Gram-negative bacterial infections.

Here, we carried out LM-metabolomics with infectious-inflammatory exudates and identified specific pro-resolving mediators that were also present in germ-free mice. RvD1 and RvD5 each accelerated resolution of *E. coli* infections and increased survival. SPM given together with ciprofloxacin shortened resolution intervals, stimulated phagocyte containment of *E. coli*, enhanced bacterial killing, and protected mice from hypothermia. These are the first actions identified for RvD5. With human macrophages, both RvD1 and RvD5 stimulated phagocytosis of *E. coli* in a GPR32-dependent manner. SPM also enhanced antibiotic effectiveness in clearing Gram-positive *S. aureus* skin infections. Together, these results indicate that stimulation of targeted host resolution responses by pro-resolving mediators in conjunction with bacterial-directed antibiotics lowers the required antibiotic doses for bacterial clearance. They illustrate new opportunities to address antibiotic resistance via lowering antibiotic use by also targeting host resolution programs.

Method Summary

Microbial-initiated inflammation in vivo

Peritonitis—Mice were given SPM or vehicle together with live *E. coli* (serotype O6:K2:H1; 10^5 or 10^7 CFU) or saline injections (mock infection) i.p. Ciprofloxacin was given 1 hr after *E. coli*. At designated points, mice were euthanized, peritoneal exudate and blood were collected. Cellular composition. intracellular *E coli*, bacterial titers and body temperatures were determined.

Resolution indices were calculated as in[4]: Ψ_{max}, the maximal PMN numbers; T_{max}, the time point when PMN reach maximum; R_{50}; 50% of maximal PMN; T_{50}, the time point when PMN reduce to 50% of maximum; R_i (resolution interval), T_{50} -T_{max}, the time period when 50% PMN are lost from exudates.

Murine dorsal skin pouches—Mice were given SPM and/or vancomycin with live *S. aureus* (serotype (b)c1; 10^5 CFU) by intra-pouch injection. Pouch exudates were collected, and bacterial counts determined. Skin punch biopsies were collected for Gram and hematoxylin-eosin staining.

Mediator-Metabololipidomics

LC/MS/MS-based LM-lipidomics were carried out using either an ABI QTrap 3200 or Qtrap 5500 (AB Sciex). LM were profiled via multiple reaction monitoring (MRM) and identified using retention time and at least 6 diagnostic ions[29].

RvD5 synthesis

RvD5 was prepared by incubating 7(R/S)-HDHA with soybean 15-LO followed by chiral HPLC separation[29]. For methyl ester preparation, RvD5 was treated with excess ethereal diazomethane and purified using reverse phase HPLC.

Macrophage and PMN phagocytosis

Human PMN or GM-CSF-differentiated MΦ were incubated with SPM or vehicle for 15 min at 37°C, followed by fluorescent-labeled *E. coli* at a 50:1 ratio (*E. coli*:MΦ) for 60 min (phagocytosis) or 120 min (gene arrays).

Statistical analysis

Statistical analyses were performed using one-way ANOVA or the Student's *t* test; $p \leq 0.05$ was taken as significant. Percent survival was analyzed by log-rank test (GraphPad).

Methods

Bacteria growth

E. coli (serotype O6:K2:H1) were cultured in LB broth and harvested at mid-log phase (OD_{600} ~0.5, 5×10^8 CFU/ml), washed in sterile saline before inoculation into mouse peritoneum.

Microbial-initiated peritonitis & leukocyte differentials

Mice were anesthetized with isoflurane and experiments were carried out with male FVB mice (6 to 8 weeks; Charles River; lab diet containing essential fatty acids from supplier). Microbial-initiated peritonitis was performed in accordance with the Harvard Medical Area Standing Committee on Animals (protocol no. 02570). Briefly, mice were anesthetized, test compounds or vehicle controls were injected into the peritoneal cavity together with live *E. coli* (10^5 or 10^7 CFU). The antibiotic ciprofloxacin (Sigma) was given 1 hour after *E. coli* injection. At designated points, mice were euthanized (overdose of isoflurane), blood was collected by heart puncture, and peritoneal exudate was collected by lavaging with 5 ml PBS. *Cellular composition*. Exudates were taken for differential leukocyte counts determined by nuclear morphology with light microscopy using Cytofuge (Statspin, Norwood, MA) stained with Wright Giemsa stain. For flow cytometry, aliquots of exudate cells were incubated with anti-mouse CD16/32 blocking Ab (0.5 μg/0.5×10^6 cells, 5 min) and then incubated (20 min, 4°C) with individual antibody or combinations of FITC-conjugated anti-mouse CD14 (clone rmC5-3) for mononuclear cells and PE-conjugated anti-mouse F4/80 Ab (clone BM8) for MΦ or PE-conjugated anti-mouse Ly-6G (clone RB6-8C5) for PMN, to determine leukocyte sub-types (FACS Canto II). Antibodies were from BD Biosciences (San Jose, CA) and eBioscience (San Diego, CA). *Intracellular E. coli levels* were determined using a FITC-conjugated anti-*E. coli* antibody (GTX40856; GeneTex). *Bacterial counts*. Aliquots of lavage or blood were used for serial dilution, plated onto LB agar plates, and cultured overnight at 37°C. *Body temperature* was monitored using an infrared thermometer (Fluke).

Resolution indices were calculated[4]: Ψ_{max}, the maximal PMN numbers in the exudates; T_{max}, the time point when PMN numbers reach maximum; R_{50}; 50% of maximal PN

numbers; T_{50}, the time point when PMN numbers reduce to 50% of maximum; R_i (resolution interval), T_{50} -T_{max}, the time period when 50% PMN are lost from the exudates.

Murine dorsal skin pouches—Pouches were raised for 6 days[30]. Mice were given test SPM and/or vancomycin with live *S. aureus* (serotype (b)c1; 10^5 CFU) by intra-pouch injection. At designated points, mice were euthanized, intra-pouch exudate and blood were collected, and bacterial counts determined. Skin punch biopsies were collected for both Gram and hematoxylin-eosin staining.

Germ-free mice

Germ-free 12-week-old C57BL/6J male mice were maintained in flexible film isolators under a 12-h light cycle and fed an autoclaved chow diet (Labdiet, St Louis, MO) *ad libitum*. Mice were sacrificed by cervical dislocation and colon were removed. All tissues were snap frozen in liquid nitrogen and stored at -80C. Animal protocols were approved by the Research Animal Ethics Committee in Gothenburg, Sweden.

Mediator-metabololipidomics

All incubations and *in vivo* samples (i.e. exudates) were stopped with two volumes of cold methanol, containing deuterated internal standards (d_8-5*S*-HETE, d_4-LTB_4 and d_4-PGE_2; Cayman Chemical, Ann Arbor, MI) were added to each sample to obtain the extraction recoveries for specific lipid mediators. Samples were taken for solid-phase extraction and LC/MS/MS-based mediator lipidomics using an HPLC-UV (Agilent 1100) coupled to an ion-trap mass spectrometer in some experiments (QTrap 3200; Applied Biosystems/Sciex); for others an ABI Qtrap 5500 equipped with a C18 column (Agilent Eclipse Plus, 4.6 mm × 50 mm × 1.8 μm) was used. The mobile phase consisted of methanol/water/acetic acid (60/40/0.01;v/v/v) and was ramped to 80/20/0.01 (v/v/v) over 5 min, to 95/5/0.01 (v/v/v) over the next 3 min and to 100/0/0.01 (v/v/v) over 6 min before returning to 60/40/0.01 (v/v/v) at a flow rate of 0.4 ml/min. Lipid mediators were profiled using multiple reaction monitoring (MRM) and identified by direct comparison with synthetic and biogenic standards using retention time and 6 diagnostic ions for matching criteria[29]. Linear calibration curves were determined using mixtures of lipid mediator standards: d_8-5S-HETE (r^2= 0.9939, n=7), d_4-LTB_4 (r^2 = 0.9995, n=7), d_4-PGE_2 (r^2 = 0.9969, n=7), RvD1 (r^2= 0.9954, n=7), RvD2 (r^2= 0.9931, n=7), RvE1 (r^2= 0.9941, n=7), LXA_4 (r^2= 0.9941, n=7), LXB_4 (r^2= 0.9959, n=7), PGE_2 (r^2= 0.8370, n=7), PGD_2 (r^2= 0.9893, n=7), 20-OH-LTB_4 (r^2= 0.9960, n=7), LTB_4 (r^2= 0.9949, n=7), PD1 (r^2= 0.9948, n=7), 17-HDHA (r^2= 0.9931, n=7), 14-HDHA (r^2= 0.9940, n=7), 7-HDHA (r^2= 0.9964, n=7), 4-HDHA (r^2= 0.9950, n=7), 15-HETE (r^2= 0.9978, n=7), 12-HETE (r^2= 0.9975, n=7), 5-HETE (r^2= 0.9905, n=7) at 50, 100, 200, 400 and 800pg. Quantification was carried out based on the peak area of the Multiple Reaction Monitoring (MRM) transition and the linear calibration curve for each. Synthetic deuterium labeled RvD1 was prepared by Dr. N. Petasis (USC) for tracking and quantitation of RvD1 in the P01(GM095467).

RvD5 synthesis and isolation

Biogenic RvD5 was prepared by incubating 7(R/S)-HDHA (Cayman Chemical) with soybean 15-LO (Sigma-Aldrich). Briefly, 7(R/S)-HDHA (50 μM) was suspended in 50mM sodium borate buffer (pH 9.3) and 1000 units of 15-LOX added. After 5 minutes, the reaction was quenched by adding the same volume of cold methanol and reduced with excess amount of sodium borohydride. Reaction mixtures were acidified and directly injected to HPLC to separate 7S,17S-dihydroxy-containing product termed RvD5. Characteristic RvD5 chromophore of lambda(max)=242nm was used for UV monitoring[29]. For methyl ester preparation, RvD5 was treated with excess ethereal diazomethane, taken to

dryness with nitrogen gas, suspended in methanol and isolated using HPLC. RvD5 reaction mixture was separated by chiral column (Chiralcel AD-RH, 150mm × 2.1mm) equipped HPLC (Agilent HP 1100 Chemstation with DAD) with gradient eluent, methanol:water:acetic acid=95:5:0.01 to 100:0:0.01 for 10 minutes at the flow rate of 200 μL/min.

Macrophage phagocytosis and gene arrays

Human MΦ were obtained by differentiating PBMC, collected from healthy volunteers, with GM-CSF (10 ng/ml) in culture medium for 7 days. Before each experiment (24 hours), cells were adhered on a 24-well plate (0.1×10^6 cells/well) in culture medium deprived of GM-CSF. In parallel, *E. coli* (serotype O6:K2:H1) harvested at mid-log phase (OD_{600} ~0.5; $\sim5\times10^8$ CFU/ml) were labeled with fluorescence dye (BacLight, Molecular Probes, Carlsbad, CA). MΦ were exposed to vehicle ($DPBS^{+/+}$) alone or compounds (PD1, RvD1, RvD5) for 15 min at 37°C, followed by incubation with fluorescent-labeled *E. coli* at 50:1 ratio (*E. coli*: MΦ) for 60 min at 37 °C. Plates were gently washed, extracellular *E. coli* quenched by trypan blue, and phagocytosis determined by measuring total fluorescence (Ex 495/Ex535 nm) using a fluorescent plate reader (Molecular Probes), and confirmed by flow cytometry (FACS Canto II).

For inflammatory gene arrays, human MΦ (2×10^6 cells) were adhered to 10-cm^2 petri dishes. Next, PD1, RvD1, RvD5 (1 nM) or vehicle was added for 15 min at 37°C, followed by addition of *E. coli* (*E. coli*:MΦ 50:1) for 120 min at 37°C. Total RNA was isolated and inflammatory gene array carried out following manufacturer's instruction (SA Biosciences). Results were analyzed using RT^2 profiler PCR array data analysis (SA Biosciences).

GPR32 receptor β-arrestin reporter system

CHO cells engineered to stably coexpress human GPR32 linked to the Pro-Link peptide and β-arrestin tagged with the β-galactosidase EA (custom constructs, DiscoveRx, Fremont, CA) denoted CHO-GPR32 were routinely grown in medium with selection antibiotics, and plated in 96-well plates (at 20,000 or 10,000 cells/well) at twenty-four hours prior to experiments. Receptor activation was determined by increased chemiluminescence upon conversion of hydrolysable substrate (PathHunter EFC Detection kit™) catalyzed by β-gal using a luminometer (Molecular Probes).

PMN phagocytosis and generation of intracellular ROS

Human PMN were obtained from healthy volunteers according to Partners Human Research Committee Protocol #1999-P-001297. Adherent human PMN (5×10^6 cells/well in a 24-well plate) were incubated with RvD5, RvD1 or PD1 (0.1-100nM) or vehicle for 15min prior to incubation with *E. coli* (JM109; 50:1 ratio) for 60 min at 37°C. Plates were gently washed, extracellular *E. coli* quenched by trypan blue, and phagocytosis determined by measuring total fluorescence (Ex 495/Ex535 nm) using a fluorescent plate reader (Molecular Probes), and confirmed by flow cytometry (FACS Canto II). To assess intracellular ROS generation, PMN (5×10^6 cells/well in a 24-well plate) were pre-incubated with 5 μM carboxy-H2DCFDA (C400; Invitrogen) for 30min, followed by incubation with SPM for 15 min, and then *E. coli* (50:1 ratio) for 60 min. Probe oxidation was determined using a fluorescent plate reader.

Statistical analysis

Results are expressed as mean ± SEM. Statistical analysis were performed using one-way ANOVA or the Student's *t* test and $p \leq 0.05$ was considered to be significant.

Supplementary Material

Refer to Web version on PubMed Central for supplementary material.

Acknowledgments

The authors thank Mary Small for expert assistance with manuscript preparation, Dr. Jim Lederer (Dept. of Surgery, BWH) for cytokine measurements, Dr. Jesmond Dalli (CET&RI, BWH) for helpful discussions, and Dr. Nicos Petasis for preparation of deuterium-labeled RvD1.

This work was supported in part by NIH grants P01GM095467 and R01GM38765 (CNS).

Abbreviations

DHA	docosahexaenoic acid
EPA	eicosapentaenoic acid
GF	Germ-free
LC-MS-MS	liquid chromatography tandem mass spectrometry
LM	lipid-derived mediators
LOX	lipoxygenase
LT	leukotriene
LX	lipoxin
PG	prostaglandins
Mϕ	macrophage
Maresins	***ma***crophage mediators in ***res***olving ***in***flammation
MFI	mean fluorescence intensity
PMN	polymorphonuclear leukocyte
PD/NPD1	protectin D1/ neuroprotectin D1, 10*R*,17*S*-dihydroxydocosa-4*Z*,7*Z*,11*E*,13*E*,15*Z*,19*Z*-hexaenoic acid
SPM	specialized pro-resolving mediators
Rv, Resolvins	bioactive omega -3 derived ***resol***ution phase ***in***teraction products
RvD1, resolvin D1:	7*S*,8*R*,17*S*-trihydroxydocosa-4*Z*,9*E*,11*E*,13*Z*,15*E*,19*Z*-hexaenoic acid
RvD5, resolvin D5:	7*S*,17*S*-dihydroxy-docosa-4*Z*,8*E*,10*Z*,13*Z*,15*E*,19*Z*-hexaenoic acid
ROS	reactive oxygen species

References

1. Houck, JC., editor. Chemical Messengers of the Inflammatory Process. Elsevier/North-Holland Biomedical Press; 1979.
2. Mantovani A, Cassatella MA, Costantini C, Jaillon S. Neutrophils in the activation and regulation of innate and adaptive immunity. Nat. Rev. Immunol. 2011; 11:519–531. [PubMed: 21785456]
3. Medzhitov R. Inflammation 2010: new adventures of an old flame. Cell. 2010; 140:771–776. [PubMed: 20303867]

4. Serhan CN. Resolution phases of inflammation: novel endogenous anti-inflammatory and pro-resolving lipid mediators and pathways. Annu. Rev. Immunol. 2007; 25:101–137. [PubMed: 17090225]
5. Stables MJ, Gilroy DW. Old and new generation lipid mediators in acute inflammation and resolution. Prog. Lipid Res. 2011; 50:35–51. [PubMed: 20655950]
6. Henneke P, Golenbock DT. Phagocytosis, innate immunity, and host-pathogen specificity. J. Exp. Med. 2004; 199:1–4. [PubMed: 14707110]
7. Rossi AG, et al. Cyclin-dependent kinase inhibitors enhance the resolution of inflammation by promoting inflammatory cell apoptosis. Nat. Med. 2006; 12:1056–1064. [PubMed: 16951685]
8. Dinarello CA. Anti-inflammatory agents: present and future. Cell. 2010; 140:935–950. [PubMed: 20303881]
9. Navarro-Xavier RA, et al. A new strategy for the identification of novel molecules with targeted proresolution of inflammation properties. J. Immunol. 2010; 184:1516–1525. [PubMed: 20032295]
10. Schif-Zuck S, et al. Satiated-efferocytosis generates pro-resolving CD11b^{low} macrophages: Modulation by resolvins and glucocorticoids. Eur. J. Immunol. 2011; 41:366–379. [PubMed: 21268007]
11. De Caterina R. n-3 fatty acids in cardiovascular disease. N. Engl. J. Med. 2011; 364:2439–2450. [PubMed: 21696310]
12. Morris T, et al. Effects of low-dose aspirin on acute inflammatory responses in humans. J. Immunol. 2009; 183:2089–2096. [PubMed: 19597002]
13. Oh SF, Pillai PS, Recchiuti A, Yang R, Serhan CN. Pro-resolving actions and stereoselective biosynthesis of 18*S* E-series resolvins in human leukocytes and murine inflammation. J. Clin. Invest. 2011; 121:569–581. [PubMed: 21206090]
14. Spite M, et al. Resolvin D2 is a potent regulator of leukocytes and controls microbial sepsis. Nature. 2009; 461:1287–1291. [PubMed: 19865173]
15. Mead PS, et al. Food-related illness and death in the United States. Emerg. Infect. Dis. 1999; 5:607–625. [PubMed: 10511517]
16. Klingensmith, ME.; Soybel, DI. The Physiological Basis of Modern Surgical Care. Miller, TA.; Rowlands, BJ., editors. Mosby Year Book; 1998. p. 478-490.
17. Xu YN, Zhang Z, Ma P, Zhang SH. Adenovirus-delivered angiopoietin 1 accelerates the resolution of inflammation of acute endotoxic lung injury in mice. Anesth. Analg. 2011; 112:1403–1410. [PubMed: 21543779]
18. Serhan CN, et al. Resolvins: a family of bioactive products of omega-3 fatty acid transformation circuits initiated by aspirin treatment that counter pro-inflammation signals. J. Exp. Med. 2002; 196:1025–1037. [PubMed: 12391014]
19. Bäckhed F, Manchester JK, Semenkovich CF, Gordon JI. Mechanisms underlying the resistance to diet-induced obesity in germ-free mice. Proc. Natl. Acad. Sci. U.S.A. 2007; 104:979–984. [PubMed: 17210919]
20. Krishnamoorthy S, et al. Resolvin D1 binds human phagocytes with evidence for pro-resolving receptors. Proc. Natl. Acad. Sci. U.S.A. 2010; 107:1660–1665. doi:doi: 10.1073/pnas.0907342107. [PubMed: 20080636]
21. Grkovich A, Johnson CA, Buczynski MW, Dennis EA. Lipopolysaccharide-induced cyclooxygenase-2 expression in human U937 macrophages is phosphatidic acid phosphohydrolase-1-dependent. J. Biol. Chem. 2006; 281:32978–32987. [PubMed: 16950767]
22. Jin SL, Lan L, Zoudilova M, Conti M. Specific role of phosphodiesterase 4B in lipopolysaccharide-induced signaling in mouse macrophages. J. Immunol. 2005; 175:1523–1531. [PubMed: 16034090]
23. Link A, Selejan S, Maack C, Lenz M, Böhm M. Phosphodiesterase 4 inhibition but not beta-adrenergic stimulation suppresses tumor necrosis factor-alpha release in peripheral blood mononuclear cells in septic shock. Crit. Care. 2008; 12:R159. [PubMed: 19091080]
24. Stables MJ, et al. Priming innate immune responses to infection by cyclooxygenase inhibition kills antibiotic-susceptible and -resistant bacteria. Blood. 2010; 116:2950–2959. [PubMed: 20606163]
25. World Health Organization. Antibiotics Resistance. Feb. 2011 Factsheet No. 1942011, doi: http://www.who.int/mediacentre/factsheets/fs194/en/

26. Seki H, et al. The anti-inflammatory and proresolving mediator resolvin E1 protects mice from bacterial pneumonia and acute lung injury. J. Immunol. 2010; 184:836–843. doi:doi: 10.4049/jimmunol.0901809. [PubMed: 20007539]

27. El Kebir D, et al. 15-epi-lipoxin A4 inhibits myeloperoxidase signaling and enhances resolution of acute lung injury. Am. J. Respir. Crit. Care Med. 2009; 180:311–319. [PubMed: 19483113]

28. Prescott D, McKay DM. Aspirin-triggered lipoxin enhances macrophage phagocytosis of bacteria while inhibiting inflammatory cytokine production. Am. J. Physiol. Gastrointest. Liver Physiol. 2011; 301:G487–G497. [PubMed: 21659618]

29. Yang R, Chiang N, Oh SF, Serhan CN. Metabolomics-lipidomics of eicosanoids and docosanoids generated by phagocytes. Curr. Protoc. Immunol. 2011; 95:14.26.11–14.26.26.

30. Winyard, PG.; Willoughby, DA., editors. Inflammation Protocols. Humana; 2003.

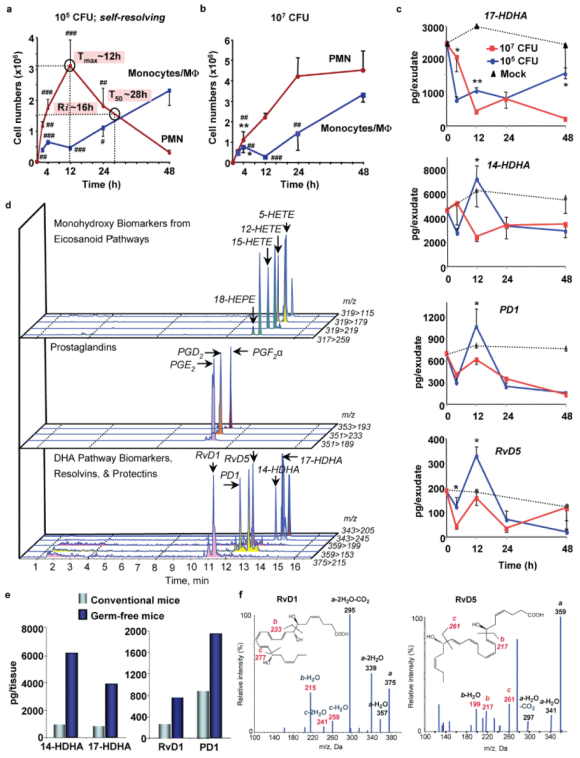

Figure 1. Profiling of SPM in *E. coli* infections

Mice were inoculated with *E. coli* at (a) 10^5 or (b) 10^7 CFU by intraperitoneal injection, and peritoneal leukocytes enumerated. Results are expressed as mean±s.e.m., n=4-6. See Methods for calculation of resolution indices. *p<0.05, **p<0.01, vs. 24h; $^{\#}p$<0.05, $^{\#\#}p$<0.01, $^{\#\#\#}p$<0.001, vs. 48h. (c) Time course of SPM and related pathway markers. Results are expressed as mean±s.e.m. of n=5 separate time courses. *p<0.05, **p<0.01, self-resolving (10^5 CFU) vs. higher titer (10^7 CFU) *E. coli* exudates. (d) Representative MRM chromatograph of eicosanoid, resolvin and protectin pathway products from naive germ-free mice. Each LM was identified based on published LC-MS-MS[30] (see Table S1). (e) SPM and pathway markers in colons of germ-free and conventional mice; representative of 3 mice. (f) Representative MS-MS of RvD1 (from germ-free mice) and RvD5 (from *E. coli*-infected mice); *a*=[M-H] (parent ion).

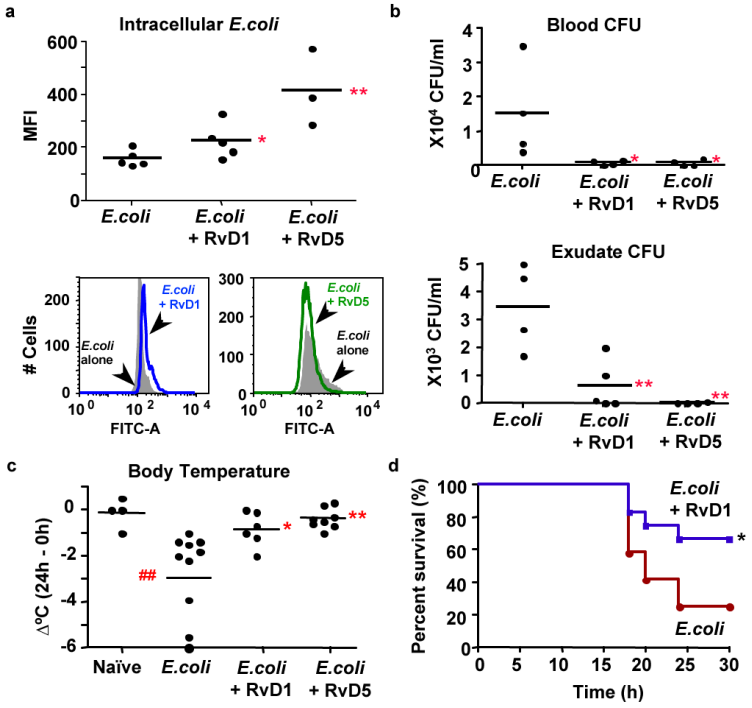

Figure 2. RvD1 and RvD5 protect mice during infection: enhancing bacterial killing and preventing hypothermia

Mice were inoculated with *E. coli* (10^7 CFU) together with RvD1 or RvD5 methyl ester (100 ng), and peritoneal exudates collected 24h later. (a) Intracellular *E. coli* levels. MFI denotes mean fluorescence intensity. Results are expressed as mean of n=3-5. (bottom panel) Representative histograms. (b) Bacterial titers. Results are expressed as mean of n=4-5. (c) Changes in body temperatures expressed as mean of Δ°C (24h-0h) n=4-10. *p<0.05, **p<0.01, vs. *E. coli* alone; ##p<0.01, vs. naïve mice. (d) % survival of *E. coli* inoculated mice (2.5×10^7 CFU) alone or with RvD1 (100 ng/mouse). *p<0.05 log-rank (Mantel-Cox) test, n=12 each group.

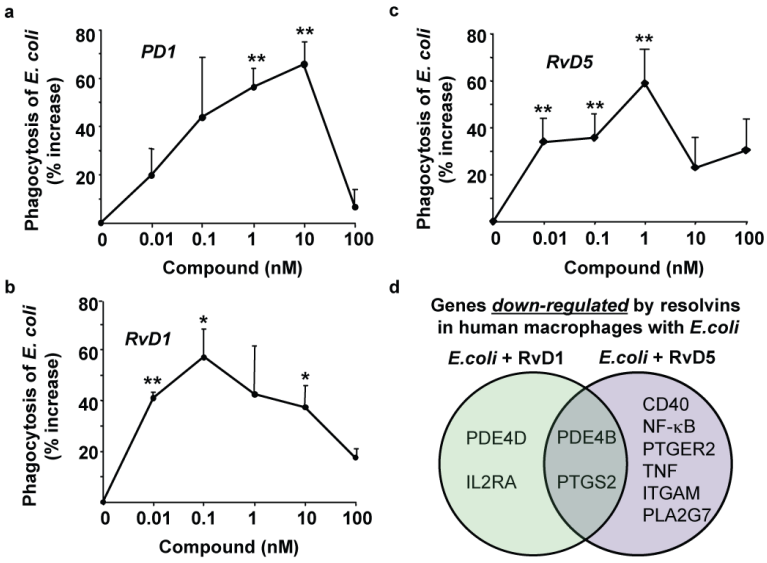

Figure 3. SPM enhance human macrophage phagocytosis of *E. coli*

(a-c) MΦ phagocytosis of fluorescent *E. coli* in the presence of PD1, RvD1 or RvD5. Results are percent increase above vehicle and expressed as mean±s.e.m., d=3-4, n=3 (PD1) or 4 (RvD1 and RvD5). **p*<0.05, ***p*<0.01, *E. coli* plus SPM vs. *E coli* alone. (b) Venn diagrams of genes regulated by resolvins in human MΦ incubated with *E. coli*. CD40 (TNFRSF5, TNF receptor superfamily member 5), ITGAM (CD11b), PDE (phosphodiesterase), PLA2 (phospholipase A2)**,** PTGS2 (cyclooxygenase-2), PTGER2 (prostaglandin E_2 receptor, EP2).

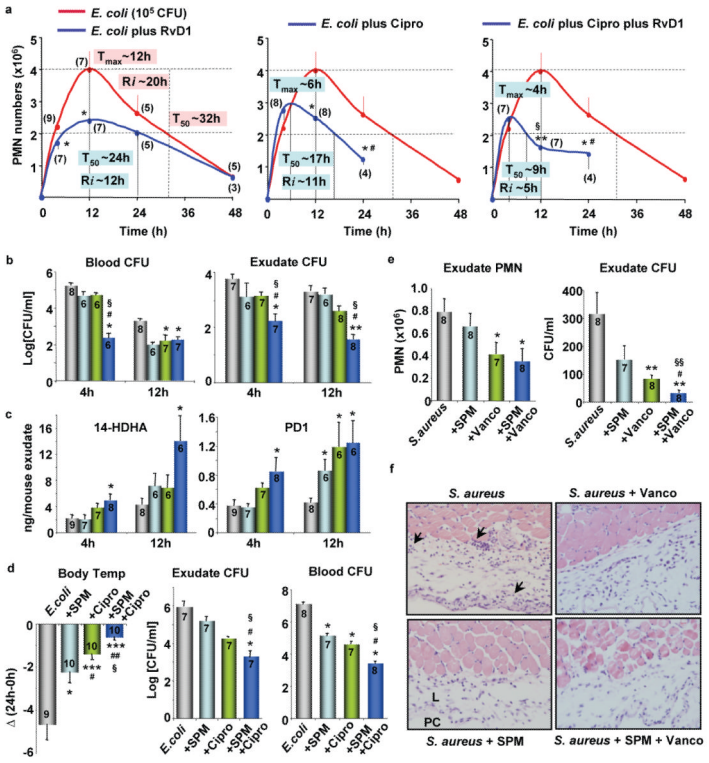

Figure 4. SPM and antibiotics accelerate resolution and enhance bacterial killing

(a-c) Mice were inoculated with *E. coli* (10^5 CFU), RvD1 methyl ester (50 ng), and ciprofloxacin (Cipro, 50 ng). (a) Exudate PMN numbers and resolution indices. (b) Bacterial titers. (c) 14-HDHA and PD1 levels determined using LC-MS-MS-based LM-lipidomics. Results are expressed as mean±s.e.m. *p<0.05, **p<0.01, vs. *E. coli* alone; $^{\#}p$<0.05, $^{\#\#}p$<0.01, vs. *E. coli*+RvD1; $^{\S}p$<0.05, vs. *E. coli*+Cipro. Gray, *E. coli* alone; blue, *E.coli*+RvD1; green, *E.coli*+Cipro; dark blue, *E.coli*+RvD1+Cipro. (d) Mice were inoculated with *E. coli* (10^7 CFU), SPM panel (RvD1, RvD5 and PD1; 50 ng each) and Cipro (25 μg). Body temperatures and bacterial titers were determined at 24h. Results are expressed as mean±s.e.m. *p<0.05, **p<0.01, ***p<0.001 vs. *E. coli* alone; $^{\#}p$<0.05, $^{\#\#}p$<0.01 vs. *E. coli*+SPM; $^{\S}p$<0.05, vs. *E. coli*+Cipro. (e,f) Murine dorsal pouches were given live *S. aureus* (10^5 CFU) alone, plus SPM (RvD1, RvD5, PD1 at 100 ng each per mouse), vancomycin (Vanco, 2.5 μg), or both SPM and vancomycin by intra-pouch injection, pouch exudates were collected at 24h. (e) PMN and bacterial counts (CFU). Results are expressed as mean±s.e.m. *p<0.05, **p<0.01 vs. *S. aureus* alone; $^{\#}p$<0.05, vs. *S. aureus*+SPM; $^{\S\S}p$<0.01, vs. *S. aureus*+Vanco. (f) Skin-pouch biopsies (Magnifications 40X). Arrows denote PMN infiltration into pouch linings. PC, pouch cavity. L, linings. Animal numbers are denoted within brackets (a) or bars (b-e).